Scientific
Research
Publishing

Temperature Fractionation (TF) of Hg Compounds in Gypsum from Wet Flue Gas Desulfurization System of the Coal Fired Thermal Power Plant (TPP)

Matej Sedlar[1,2], Majda Pavlin[2,3], Radojko Jaćimović[3], Andrej Stergaršek[4], Peter Frkal[3], Milena Horvat[2,3]*

[1]Esotech, d.d., Velenje, Slovenia
[2]International Postgraduate School Jožef Stefan, Ljubljana, Slovenia
[3]Jožef Stefan Institute, Ljubljana, Slovenia
[4]KEMEK d.o.o., Ljubljana, Slovenia
Email: *milena.horvat@ijs.si

Abstract

Gypsum from the wet flue gas desulfurization system of the lignite fired thermal power plant Šoštanj, Slovenia, can efficiently retain mercury (Hg), of which most is contained in finer gypsum fractions, with concentrations above 10 kg⁻¹. The aim of this work was to identify and study the temperature stability of Hg species in gypsum by a temperature fractionation (TF) method. A self-constructed apparatus was used that consisted of an electrical furnace for controlled heating up to 700°C, with a heating rate of 2.2°C·min⁻¹, and an AAS detector with Zeeman background correction. The pattern of Hg release during temperature increase depends highly on the matrix/substrate in which it is contained. Based on spiking gypsum with known Hg compounds we concluded that the largest proportion of Hg in gypsum belongs to Hg-Cl and Hg-Br compounds appearing at 160°C to 200°C, followed by smaller amounts of HgO, HgS and Hg sulfates appearing at 300°C and 450°C. Further development of methodology for identifying Hg species would require identification of the decomposition fragments of Hg and other compounds, complemented by a better understanding of Hg reactivity at higher temperatures.

Keywords

Temperature Fractionation, Mercury Compounds, FGD Gypsum, Multi-Element Analysis, Spiking

---

*Corresponding author.

1. Introduction

Mercury (Hg) is a global pollutant, the main source in the atmosphere being the combustion of fossil fuels in particulate coal burning and other high temperature industrial processes [1]. One of the main objectives of the recently adopted Minamata Convention [2] is to reduce Hg emissions into the environment. More stringent emission standards for Hg are therefore expected in the near future, and much effort is focused on developing efficient and economically acceptable technologies for Hg removal. Flue gas released from coal combustion contains elemental Hg (Hg(0)), oxidized Hg(II) and Hg bound to particles, Hg(P) [3] [4]. Hg(P) could be retained in electrostatic precipitators (ESP) or baghouses, while Hg(0) and Hg(II) remain predominantly in the gaseous phase of the flue gas [4]. Hg could be oxidized in the gas phase on particles (e.g. active carbon) over a selective catalytic reduction unit (SCR) [5], in interaction with different gases or in a wet flue gas desulfurization (WFGD) system. Oxidized Hg is much more soluble in water than Hg(0) and could therefore be effectively removed in wet scrubbers.

WFGD scrubbers are very efficient in reducing SO_2 emissions and, simultaneously, retain Hg(II), however oxidation of Hg(0) to Hg(II) is also possible under appropriate conditions (temperature, pH, Eh, additives and others compound present, etc.) [6]-[8]. Oxidation of Hg(0) is much more efficient when a prior SCR unit is installed [9]. Additionally, reduction of Hg(II) into Hg(0) was observed, which can lead to re-mobilization of oxidized Hg into the gaseous phase and increased emissions into the atmosphere [4]. Other contaminants, originating from coal (As, Se, etc. [10]-[13]), could be present in FGD slurry and are partitioned between solid by-products (e.g. gypsum) and water solution. In general, all the ions present in the slurries of WFGD plant affect the chemistry and stability of Hg and Hg species [14]-[16]. Some additives are very successful in Hg oxidation therefore it is very important during the disposal to be aware of the toxic products they contain [8] [17]. Finally, most of the WFGD wastes are landfilled but some portion is used for wallboard production [18]-[21], as an additive to cement and concrete production and as a soil amendment [19]. The amount of Hg released from wallboard production at the temperature where this process begins is very important in developing efficient production without Hg re-emission.

Generally, various Hg compounds are present in gypsum and in solid samples. Recently, their presence has been determined with various methods such as the leaching test [22] [23] and thermal fractionation [24]-[33]. Hg compounds have different properties, including different vapor pressures at different temperatures [18]. This is why the temperatures at which Hg compounds are decomposed and evaporated are different. Therefore, investigations of thermal stability of Hg compounds in different solid samples are of interest, and, for two reasons: i) to understand temperature stability of Hg in solid substrates/wastes and ii) to define Hg fractions released during controlled heating as proxies for the identification of Hg compounds present in solid substrates. However, as evident from the literature [22] [30] [34]-[36], the experimental conditions (amount of sample, heating rate, flow rate, gas type, presence of substrate mixed with Hg compounds…) may contribute to the differences between published results. Calibration with pure Hg compounds may be of help, although properties of solid substrates may affect the breakdown process and appearance of Hg peaks at different temperatures [36]-[39].

Retention of Hg in WFGD slurry and consequently the latter's stability is very important. Hg could be partitioned between the solid (gypsum, unconsumed limestone, insoluble constituents of limestone and solids washed out of the flue gas) and aqueous phases, and has the affinity for retention in the finer fractions. The particle size and porosity of gypsum are very important in partitioning Hg between phases. Limestone that is added continuously into scrubber contains Mg (as dolomite, $CaMg(CO_3)_2$), Si (quartz, SiO_2), Fe, Mn, Al and other metals [40]. For example, 12% of total gypsum mass contains 62% of its Hg bound on small particles [6]. Gypsum slurry settles in two layers, upper brownish slowly-settling and bottom white-grey layers. The upper layer contains much more Hg and is also enriched with Si, Al, Fe, Mg and some trace elements such as Ti, Mn and Ba [41]. Thermal and dissolution stability can vary between Hg compounds and complexes in the gypsum. Knowledge about the interactions of Hg, ligands, metals and particles present in WFGD slurry is very important. When considering sorption properties, the well-known correlation of Hg and Fe as iron oxyhydroxides, could also be present [42]. There is evidence showing increased Hg concentration in the solid fraction when Fe species are available in the slurry. Probably, Fe is introduced with the lime or limestone added to the WFGD scrubber, where it can be found as Fe-coated clay minerals or Fe-oxide/hydroxide particles [41]. Kim *et al.* [43] showed a correlation between Fe and Hg where an additional leaching test described strong chemical sorption rather than physical adsorption of Hg. The importance of ligands (chloride, sulfate) presents in solutions that increase/decrease the Hg sorption to mineral sorbents such as goethite (α-FeOOH), γ-alumina (Al_2O_3) and bayerite (β-

$Al(OH)_3$) has also been demonstrated [43].

Furthermore, during some extraction experiments in gypsum and wallboard production, a major Hg-releasing step—and therefore possible minerals of Hg-binding material—was also revealed. Fe, Al, K, Mg, Si, and S were the most common elements, indicating some of the minerals responsible for affecting the Hg-adsorption—iron oxides, iron hydroxide, phyllosilicate minerals (illite $(K,H_3O)(Al,Mg,Fe)_2(Si,Al)_4O_{10}[(OH)_2,(H_2O)]$, glaucoite $(K,Na)(Fe^{3+},Al,Mg)_2(Si,Al)_4O_{10}(OH)_2$) and iron sulfides [19]. X-ray diffraction analysis confirmed the presence of phyllosilicate minerals (illite and kaolinite $(Al_2Si_2O_5(OH)_4)$) in post-leaching gypsum and wallboard residues [42]. Limestone that is introduced into a WFGD system contains only little of these minerals [44].

The effect of a WFGD system on Hg retention is clearly evident in the thermal power plant (TPP) in Šoštanj, Slovenia where the retention of total Hg in the WFGD is as high as 89% [6]. The results of research reported here shows that the majority of Hg is retained in the slow-settling, finer particulate phase of the WFGD, with concentrations exceeding values of 10 mg·kg^{-1} of Hg.

TPP Šoštanj consists of five power blocks with combined power of 779 MW. As a fuel it uses lignite from the local mine with a heating value of 9.5 MJ·kg^{-1} and a consumption rate between 3.5 and 4.2 million tons per year. TPP Šoštanj has 2 WFGD units installed for removing sulfur oxides, the first covering blocks 1 to 4 and the second just block 5, both units using the wet limestone process with forced oxidation [6] [45].

The aim of this work was to study the temperature stability of Hg and to identify the Hg compounds present in gypsum from Šoštanj TPP. Multi-element analyses of gypsum samples and Velenje lignite were also conducted in order to assist interpretation of the results. The processes of Hg retention in the WFGD have recently been studied in detail [6]-[8], but have not so far included gypsum. The present paper adds to the knowledge of Hg behavior in the TPP with its high retention in the WFGD.

2. Materials and Methods

To achieve the objectives of better understanding the temperature stability of TPP gypsum samples from Šoštanj TPP, several methodological approaches have been taken to identifying Hg compounds. TPP gypsum samples were analyzed using the temperature fractionation method. Pure Hg compounds mixed with $CaSO_4·2H_2O$ substrate were prepared, as calibration standards and to study the effect of solid substrate on the temperature stability of the Hg compounds. These mixtures were then added to Šoštanj TPP gypsum in order to observe the effects of matrix on the temperature at which Hg compounds were released from the samples.

Multi-element analysis in different fractions of the gypsum and lignite samples was also performed.

2.1. Sample Preparation

2.1.1. Preparation and Characterization of the Gypsum Samples

Particles in 3 liters of the WFGD slurry from TPP Šoštanj were first separated into fine and coarser fractions labelled as FF and CF, with the help of a hydro cyclone. Half of the FF was returned into the separation process, where it was again separated into fine and coarser fractions labelled as FF1 and FF2. Four different size fraction samples were thus obtained in which FF contains both granulation sizes of FF1 and FF2. Granulation analyses of gypsum samples were conducted with Microtrac PSA FRA 9200 based on Fraunhofer laser diffraction. The size distribution of particles in each sample is presented in **Figure 1**.

Samples were then oven dried at 38°C for a week to constant weight, in an electric drier/oven MEMMERT UFE 500. Moisture content lost during drying was 7.9% for FF, 8.7% for FF1, 3.2% for FF2 and 4.8% for sample CF.

After drying, samples were homogenized in the agate containers of a planetary mill (Fritsch planetary mill Pulverisette 7).

An aliquot of the original gypsum sample (not oven dried) was also kept for studies of the potential influence of moisture on Hg release during the temperature fractionation process.

2.1.2. Preparation of Samples of Pure Hg Compounds

Mercury compounds chosen for examination are presented in **Table 1**.

2.1.3. Preparation of Pure Hg Compounds Mixed with $CaSO_4·2H_2O$

These pure compounds were "diluted" by mixing with $CaSO_4·2H_2O$ powder (Sigma-Aldrich Co. LLC.; purity
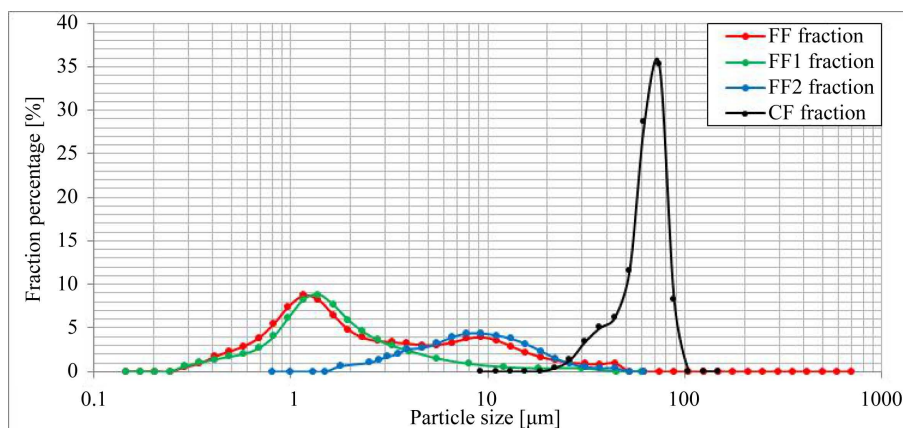
Figure 1. Size fractions of TPP gypsum samples.

Table 1. Type of mercury compound, suppliers and purity.

Mercury compound	Supplier	Declared purity
Hg_2Cl_2	Sigma-Aldrich Co. LLC.	≥99.5%
$HgCl_2$	Kemikad.d., Zagreb	99%
HgO-Red	Sigma-Aldrich Co. LLC.	≥99.5%
HgO-Yellow	May & Baker Ltd.	≥99.5%
HgS-Red	Mallinckrodt Chemical Works	99%
HgSe	Sigma-Aldrich Co. LLC.	99.9%
Hg_2SO_4	Sigma-Aldrich Co. LLC.	98%
$HgSO_4$	Sigma-Aldrich Co. LLC.	≥99%
HgF_2	Sigma-Aldrich Co. LLC.	97%
$HgBr_2$	Sigma-Aldrich Co. LLC.	98%

99% - 101% based on anhydrous substance). This substrate resembles gypsum from the WFGD in coal burning power plants. Each pure Hg compound (10 - 12 mg) was added to 5 g of substrate powder. The mixtures were carefully homogenized by mixing in zirconium containers placed in a planetary mill (Fritsch planetary mill Pulverisette 7). Homogenization was achieved in short mixing intervals of 10 minutes in order to avoid increase of temperature. The bulk homogeneity of each mixture sample (80 - 140 mg) was checked by wet digestion of 6 independent analyses of total Hg, followed by Hg determination by cold vapor atomic absorption spectrometry (CV AAS) after reduction with $SnCl_2$ [46].

2.1.4. Preparation of Gypsum Samples Spiked with Pure Mercury Compounds Mixed with $CaSO_4 \cdot 2H_2O$

Only the sample with the highest Hg content (sample FF) and finer particle size was chosen. It was spiked with ten different pure Hg compounds (**Table 1**), each previously mixed with $CaSO_4 \cdot 2H_2O$ (1 - 7 mg). The mixtures were placed in a planetary mill (Fritsch planetary mill Pulverisette 7) for several homogenization periods of 10 minutes.

2.1.5. Preparations of Lignite Samples

Lignite samples were obtained at random from a conveyer belt during a normal working day to ensure representative samples. The combined mass of the samples was around 3 kg. They were dried to constant weight at 38˚C for a week in an electric drier/oven MEMMERT UFE 500. After the drying process, the combined samples

were ground with a ball mill and sieved with a Fritsch Pulverisette 0 Vibratory Micro Mill to a particle size of less than 250 µm.

2.2. Multi-Element Analysis of Gypsum and Lignite Samples

For k_0-instrumental neutron activation analysis (k_0-INAA) an aliquot (varied from 0.1 to 0.26 g) of gypsum and lignite samples was sealed into a pure polyethylene ampoule (SPRONK system, Lexmond, The Netherlands). Determination of short lived radionuclides was conducted by staking an aliquot and standard Al-0.1% Au (IRMM-530R) together, fixed in the polyethylene vial in sandwich form, and irradiated for 5 minutes in the carousel facility of the TRIGA reactor with a thermal neutron flux of 1.1×10^{12} cm^{-2}·s^{-1}. For determination of medium and long lived radionuclides an aliquot and standard Al-0.1% Au were prepared on the same way as already described above for the short lived radionuclides. In this case irradiation lasted for 12 hours and was conducted in the carousel facility of the TRIGA reactor as well.

When short irradiation (5 minutes) was completed, the aliquot was measured after 10 and 35 minutes cooling time on absolutely calibrated HPGe detectors with a 40 and 45% relative efficiency. After long irradiation (12 hours) the aliquot was measured after 4, 8, and 20 days cooling time on the same HPGe detectors. For peak area evaluation, the HyperLab 2002 program was used. The values f = 28.63 (thermal to epithermal flux ratio) and α = –0.0011 (epithermal flux deviation from the ideal 1/E distribution) were used to calculate element concentrations [47] [48]. Software package Kayzero for Windows was applied [49] to calculate the elemental concentrations and effective solid angle.

The k_0-INAA procedure is accredited according to ISO/IEC 17025:2005 by the Slovenian Accreditation Agency (Accreditation certificate LP-090).

2.3. Experimental Apparatus for Temperature Fractionation

2.3.1. Apparatus

An RA-915+ Hg Analyzer with a PYRO-915+ pyrolysis unit was used for the detection of Hg. The instrument was developed for direct determination of total Hg by combustion of samples and cold vapor atomic absorption detection (CV AAS) with Zeeman background correction [50].

The apparatus used for temperature fractionation was a home-constructed device (**Figure 2**). It consists of a
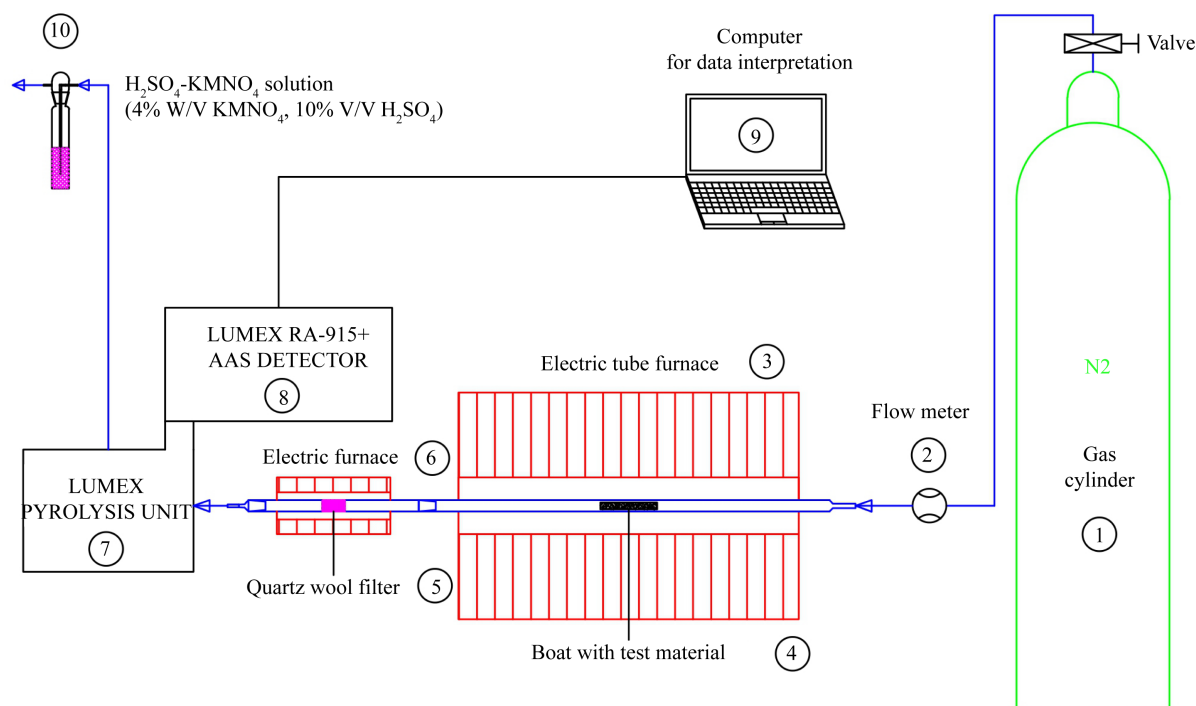

Figure 2. Scheme of the measuring line.

gas tank (1) for the supply of carrier gas, a flow meter (2) for flow adjustment and quartz tubes. The first quartz tube, with an outer diameter of 20 mm and inner diameter of 16 mm, was placed in the electric tube furnace (3). The quartz boat used for samples (4) was carefully positioned in the first quartz tube in the middle of the electric tube furnace Nabertherm RT 50/250/11 where the thermocouple is located. The quartz boat is semi-circular, with an inner diameter of 5 mm and length of 35 mm. The tube furnace consists of a ceramic tube, inner diameter 50 mm, and two plugs of ceramic fiber on each side. Each plug has a drilled hole in the middle for a tight fit to a quartz tube to reduce heat loss. The second quartz tube, with same dimensions as the first, was packed with quartz wool (5) and heated to 700°C in a small electric furnace with inner diameter of 27 mm (6) to ensure the transformation of all volatile Hg compounds to elemental Hg and to retain any particles that may be released from the sample. The Lumex Pyro 915+ pyrolysis unit, with dimensions of $350 \times 350 \times 120$ mm (7), ensured additional decomposition of any remaining volatile compounds of Hg that might interfere with the atomic absorption measurement [50]. Elemental Hg was detected by the Lumex Ra-915+ atomic absorption detector with Zeeman correction with detector dimensions of $470 \times 210 \times 110$ mm (8), which was connected directly to a computer (9) for data collection. An impinger containing H_2SO_4-$KMnO_4$ solution (10) was connected to the exhaust from the Lumex Ra-915+ to retain Hg(0) in solution by oxidation.

2.3.2. Procedure

Around 50 mg of each gypsum sample (FF, CF, FF1 and FF2) and each spiked FF sample was weighed in a quartz boat. When pure Hg compounds mixed with $CaSO_4 \cdot 2H_2O$ were tested only 10 - 30 mg of the sample was weighed into the sample boat and as small amount of pure Hg compound as possible, not to exceed the upper limit of the detection range (2 - 30,000 ng·m^{-3}) [50]. However, for a signal to even be recognized as a peak of released Hg, at least 20 ng of Hg should be present in the sample—due to noise caused by the detector Lumex Ra-915+. The results of mass balance for different samples showed that the intensity of the peaks does not match perfectly to recording units (ng·m^{-3}), due to a drifting measuring baseline, as a software deficiency. However, these units serve for easier comparison of the signal intensity. To resolve the drifting baseline problem, corrections were made on every thermogram by deducting the thermogram area, obtained by averaging several thermograms of blank samples. In addition to baseline correction, temperature correction was also considered, due to difference in the temperature measured at the sample and that recorded by the electric tube furnace (**Figure 2**, (3)). An independent measuring thermocouple was fused directly into the quartz tube, where the sample is located, giving precise temperature readings. After several experiments, the average of the temperature data was calculated and deducted from the data recorded by electric tube furnace to provide correct temperature. The sample boat (**Figure 2**, (4)) was carefully positioned in the middle of the quartz tube which was heated from room temperature to 700°C with a linear heating rate of approximately 2.2°C·min^{-1}. Nitrogen (99.996%) was used as a carrier gas to flush Hg vapor released from the sample through the measurement train at a flow rate of 1 L·min^{-1}. To verify that the peaks, shown on computer, really belong to Hg release, impingers were changed before every peak release and content was measured to determine retained Hg concentration.

2.3.3. Data Interpretation

To receive correct readings, the pyrolysis unit (**Figure 2**, (7)) has several different setting modes to choose the most appropriate gas flow rate and heating temperatures according to the type of a given sample. In our case, mode 1, using a gas flow rate of 0.8 - 1.2 L·min^{-1} and the atomizer at 680°C - 740°C was selected, which suits sample materials such as soils, sediments, ores, coal and minerals. Data are interpreted by the Lumex software as a signal for continuous measurement of the concentration in ng·m^{-3} shown on the ordinate axis as a function of time in seconds displayed on the abscissa axis. Due to known heating rate and precise temperature readings, the concentration signal per time was adapted to a concentration signal per degree temperature, °C, to observe Hg release on increment of temperature.

2.3.4. Total Hg in Samples

For quantitative determination of Hg in gypsum samples, around 0.5 g of sample was digested in acid solution of HNO_3-$HClO_4$ in a ratio of 1:1 (2% v/v) and H_2SO_4 (5% v/v) in Milli-Q water at 240°C for 20 minutes. Hg content was then determined by the CV AAS method (Automatic Hg Analyzer Model Hg-201, Sanso Seisakusho Co., LTD). For every sample at least two replicas were prepared and measured. For testing the homogeneity

of samples, the same procedure was used for 6 replicas, to check the repeatability of the measured Hg concentration.

2.3.5. Mass Balance

Hg released from the sample during temperature fractionation was trapped into impinger solution (4% W/V $KMnO_4$, 10% v/v H_2SO_4 in Milli-Q water) placed at the exit of a Lumex detector (**Figure 2**, (7)). The permanganate solution was sequentially pre-reduced with $NH_2OH \cdot HCl$ to destroy the excess of potassium permanganate. An aliquot of the sample was reduced to Hg(0) with an acid solution of 10% $SnCl_2$ and determined by CV AAS (Automatic Hg Analyzer Model Hg-201, Sanso Seisakusho Co., LTD) [46]. The quantity of Hg released from the sample was used to assess the mass balance, by comparing the amount of Hg contained in solid sample aliquots and the amount trapped in the impingers.

3. Results and Discussion

This section is organized in two parts, in which the first discusses the results of multi-element analysis in gypsum samples from the TPP Šoštanj and the second part the results of thermal fractionation analysis. The results of the latter are divided into two sub-sections the first of which contains results presented as thermograms of different TPP gypsum samples from TPP Šoštanj (FF, FF1, FF2, CF) (**Figure 3**) and the second, results in thermograms of TPP gypsum samples spiked with pure Hg compounds mixed with $CaSO_4 \cdot 2H_2O$ (**Figures 4-7**).
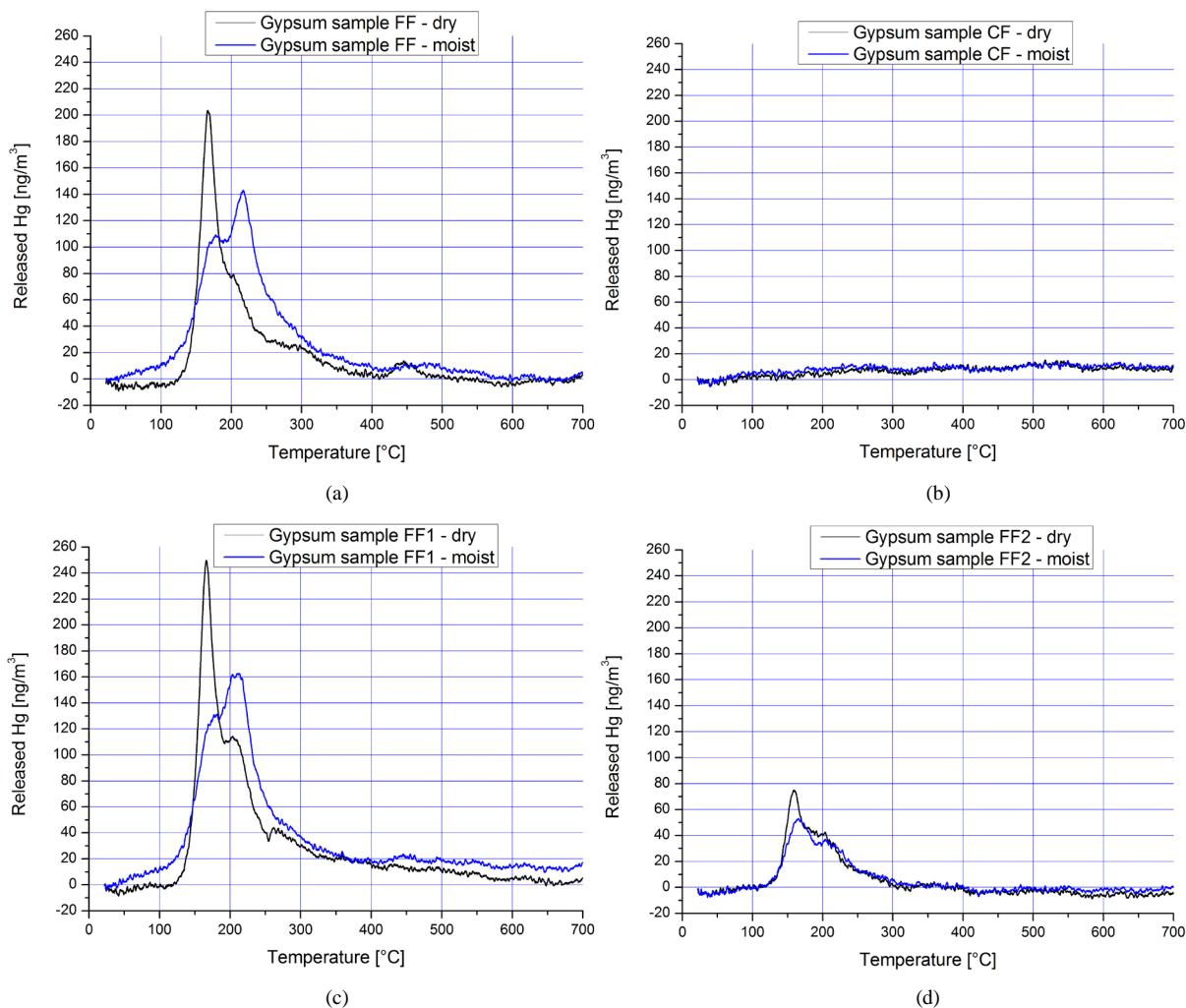

Figure 3. Thermograms of a dry and moist gypsum samples FF (a), CF (b), FF1 (c) and FF2 (d).
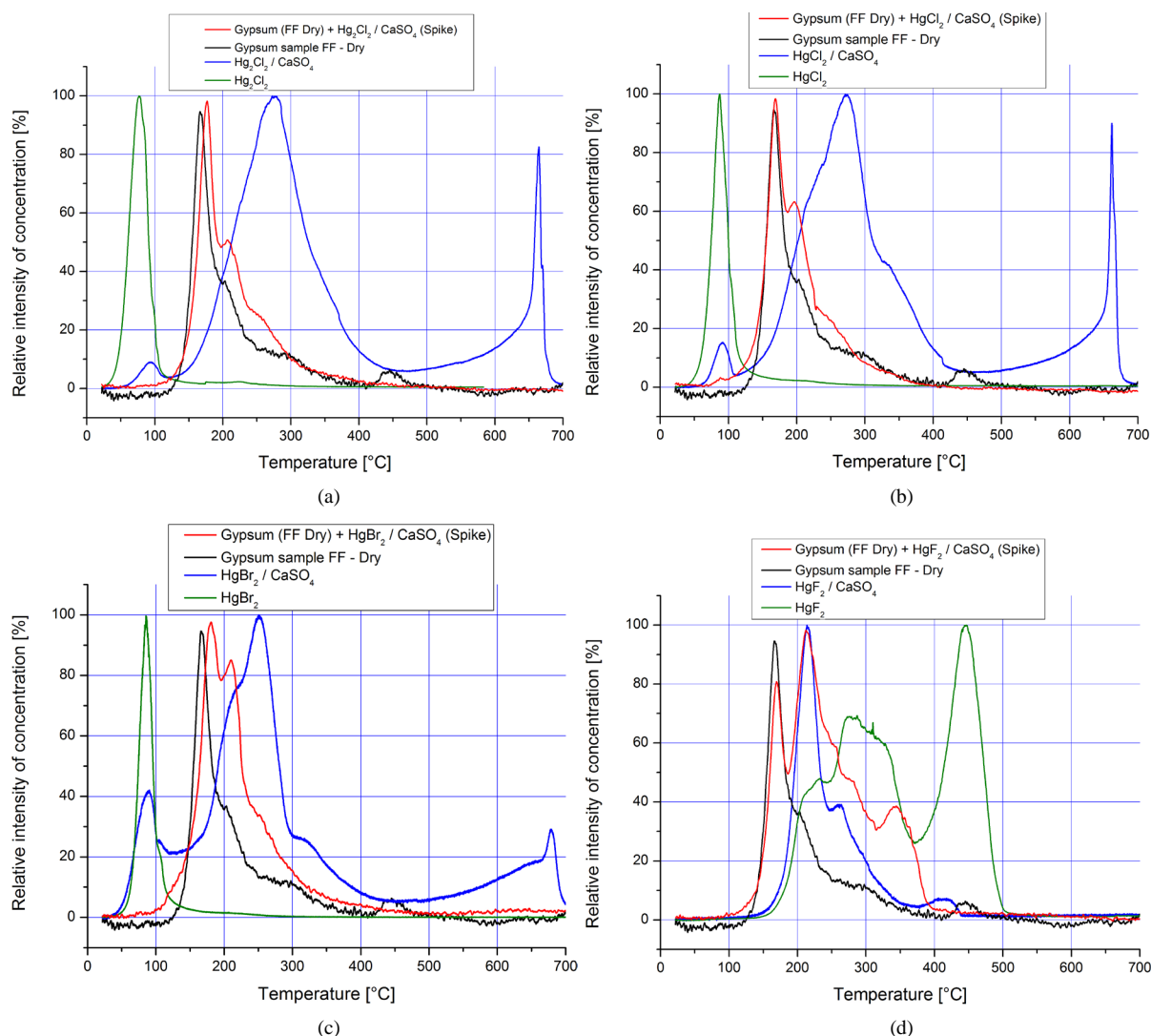
Figure 4. Thermograms of Hg_2Cl_2 (a), $HgCl_2$ (b), $HgBr_2$ (c) and HgF_2 (d) spikes.

3.1. Multi-Element Composition of Gypsum and Lignite Samples

The results for different size fractions of gypsum and for lignite are presented in **Table 2**. From **Table 2** and **Figure 8(a)** and **Figure 8(b)**, it is evident that the highest concentrations of most elements are found in the finer fractions of gypsum (FF and FF1). In FF2 sample, the ratio of elements is lower, by factor of around 2, than those the finer fractions. This is proportional to the size fraction difference (**Figure 1**). This is in agreement with earlier reports [6].

The concentration ratios between finer fractions compared with a coarser fraction (**Figure 8(a)** and **Figure 8(b)**) provide an interesting observation on partitioning of elements in the different size fractions. The elements such as Br, Ca, Sr, and Cl (**Figure 8(a)**) show smaller accumulation in fine fractions, which is due to the fact that the calcium, sulfate, chloride, and bromide represent the major components of the solids in the WFGD system. The largest concentration factors can be observed for aluminum (**Figure 8(a)**) and europium (**Figure 8(b)**). Aluminum enters the WFGD with calcite and is known to form colloids in WFGD suspension [6]. The concentration of europium is very low in all fractions especially in CF therefore the ratio is high. Other elements, belonging to different groups in the periodic system with different chemical properties show surprisingly similar concentration factors (30 to 70) indicating similar mechanisms. Prevailing mechanism which is responsible for such course of reactions is most probably the adsorption. As the salts of alkali and earth alkali elements have
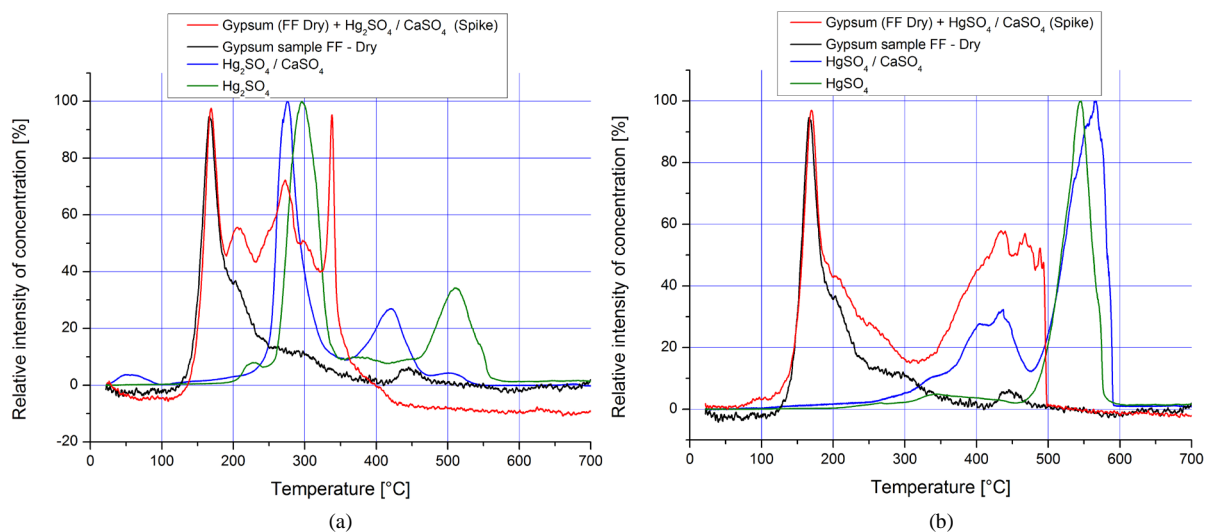
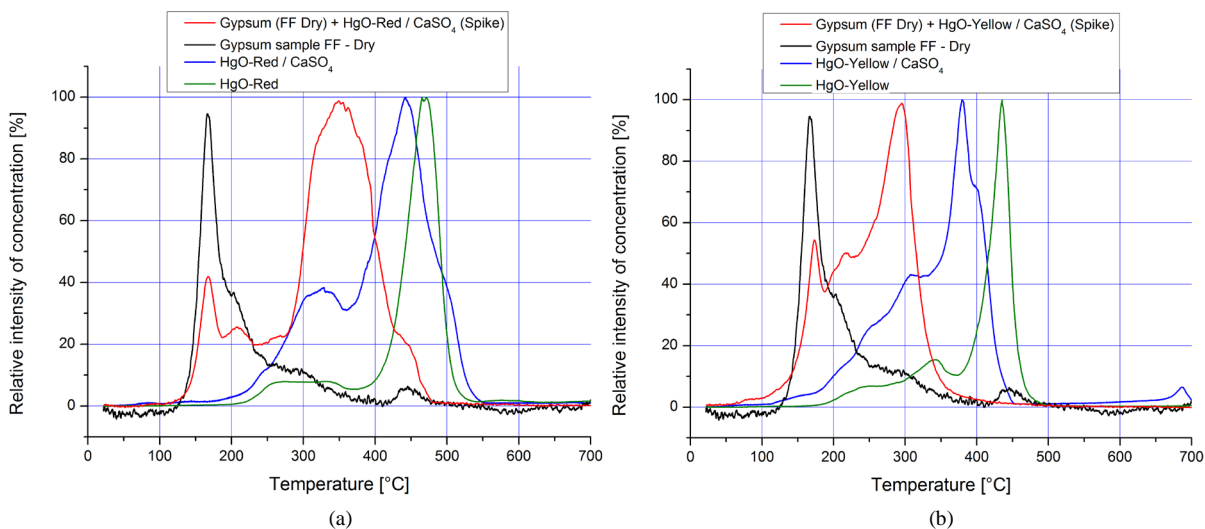**Figure 5.** Thermograms of Hg_2SO_4 (a) and $HgSO_4$ (b) spikes.

Figure 6. Thermograms of HgO-red (a) and HgO-yellow (b) spikes.

solubility several orders of magnitude higher that the salts of the transition elements, the precipitation reactions alone cannot explain these findings.

3.2. Temperature Fractionation Experiments

The results obtained by the temperature fractionation method are shown in two sections, of which the first (section 2.1.) summarizes the results obtained for different size fractions (FF, FF1, FF2 and CF) of TPP gypsum samples. As explained in the experimental section, dried and moist samples were studied and the results are shown in the eight thermograms presented in **Figure 3**.

In 2.2 are described and discussed the results of temperature fractionation for the fine fraction (FF) only and spiked with ten different pure Hg compounds, previously mixed with $CaSO_4 \cdot 2H_2O$ (**Figures 4-7**).

3.2.1. Temperature Fractionation of Gypsum Samples

The amount of the sample taken for temperature fractionation varied between 50 to 57 mg. Corresponding Hg content is given in **Table 3**, which also provides information on Hg recovered in the $KMnO_4$ impingers.

Every sample of a gypsum size fraction was measured at least twice. Mercury recovered in $KMnO_4$ impingers
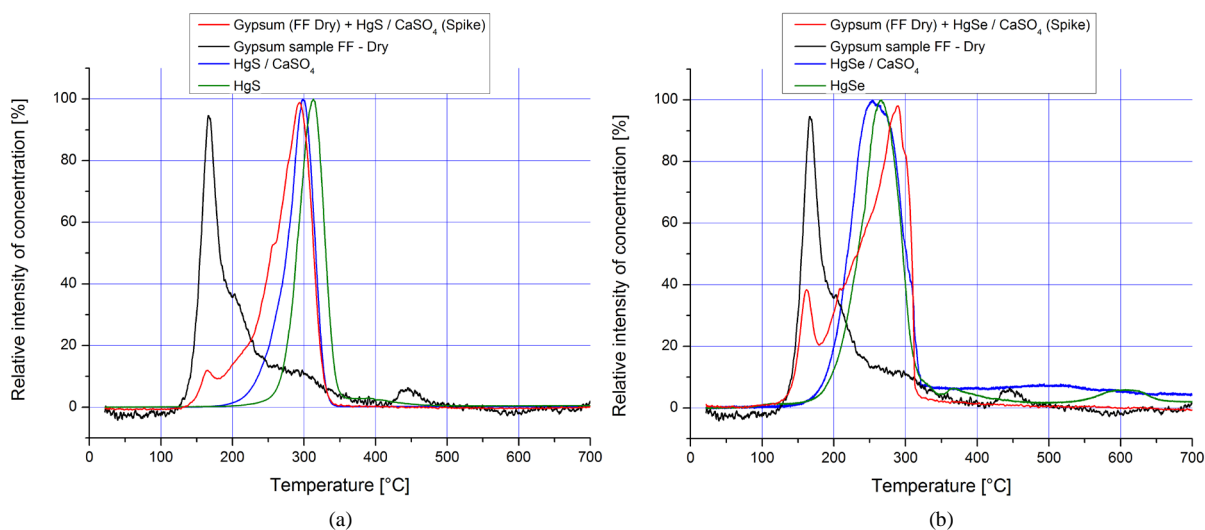
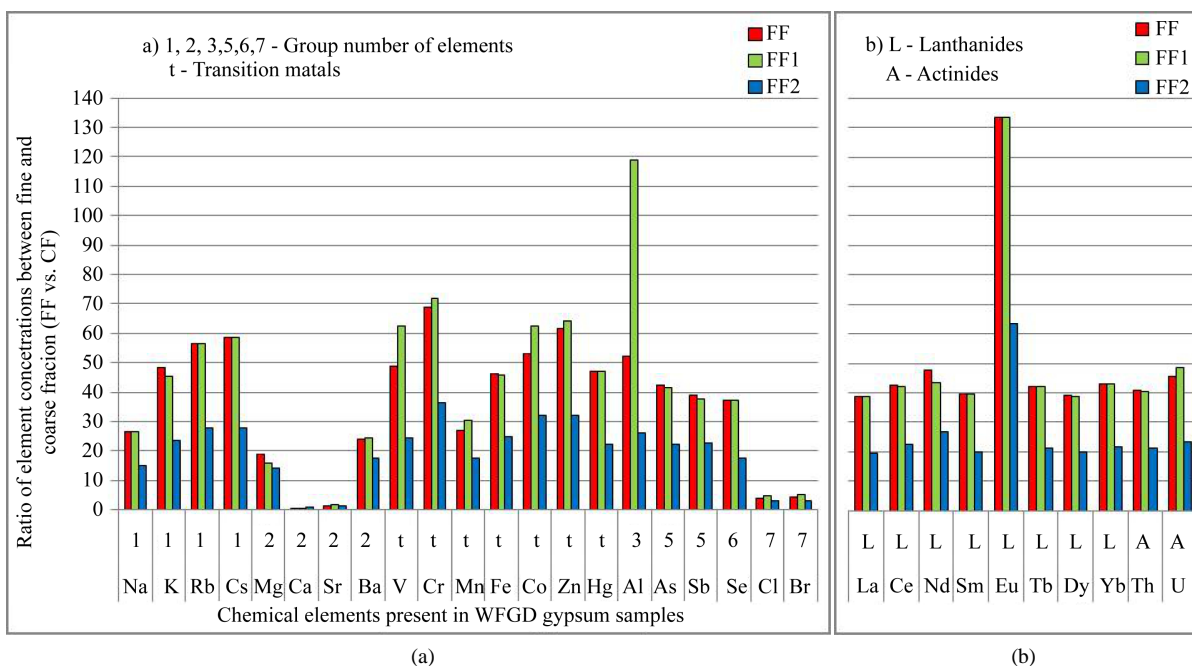**Figure 7.** Thermograms of HgS (a) and HgSe (b) spikes.

Figure 8. Concentration ratios of different elements in finer fractions (FF, FF1 and FF2) compared to coarse fraction (CF) fraction. Labels at the columns mark a group of element in the periodic table of elements.

ranged between 90% and 120%.

The results of the gypsum samples separated by granulation are shown as thermograms of concentration in ng·m^{-3} of released Hg in the carrier gas versus temperature (**Figure 3**).

Evidently, dry gypsum sample FF (**Figure 3(a)**) exhibits the most distinctive peaks with a maximum temperature of 160°C, followed by a smaller peaks at 200°C, 290°C and 440°C. The thermogram of CF does not show any peaks of Hg release (**Figure 3(b)**) due to low Hg concentration. The intensity of Hg peaks in fine fractions corresponds to the concentrations of Hg in gypsum samples.

A slight difference in the pattern is seen between those for dry and moist FF and FF1 samples (**Figure 3(a)** and **Figure 3(c)**). The first peak, at temperature of less than 200°C, is lower in the moist sample than in the dry one. It seems that humidity affects Hg release from moist samples; it is less likely that the structural changes in

Table 2. Results of multi-element analysis for dried gypsum and lignite samples obtained by k_0-INAA (Values marked as "<" fall under the limit of detection).

Sample code	FF	FF1	FF2	CF	Velenje Lignite
El.	[mg·kg⁻¹]	[mg·kg⁻¹]	[mg·kg⁻¹]	[mg·kg⁻¹]	[mg·kg⁻¹]
Ag	<0.42	<0.54	<0.25	<0.14	<0.24
Al	52,140	119,000	26,215	1001	22,156
As	39.4	38.8	20.6	0.93	8.19
Au	<0.0022	<0.003	0.0016	<0.0005	<0.0015
Ba	262	267	194	11	122
Br	35.1	41.7	26.3	8.01	6.19
Ca	144,100	140,400	193,000	222,600	19,392
Cd	9.58	11.2	6.32	<0.4	<1.0
Ce	40.6	39.8	21.2	0.95	14.5
Cl	568	683	435	147	69.9
Co	8.39	9.93	5.12	0.159	3.07
Cr	178	185	93.8	2.58	20.8
Cs	10.4	10.4	5.00	0.18	3.26
Dy	5.82	5.76	2.95	0.149	<0.7
Eu	1.20	1.20	0.57	<0.009	0.31
Fe	33,700	33,300	17,930	726	15,605
Ga	25.1	26.2	11.8	<0.66	<1.6
Hf	1.50	1.39	0.84	0.043	0.66
Hg	**10.6**	**10.5**	**5.02**	**0.22**	**0.12**
I	22.5	23.9	16.0	3.14	<10
In	0.090	0.093	0.046	<0.004	/
K	14,467	13,618	7032	299	2889
La	29.1	29.1	14.8	0.75	7.34
Mg	36,530	30,320	27,413	1920	4158
Mn	207	235	135	7.68	597
Mo	3.87	3.01	2.32	<0.52	11.3
Na	1570	1576	881	58.9	1366
Nd	25.2	23.1	14.1	<0.53	6.92
Rb	97.9	98.1	48.4	1.73	25.5
Sb	4.68	4.53	2.72	0.12	2.07
Sc	11.1	11.1	5.57	0.246	3.74
Se	87.0	87.8	41.6	2.35	0.79
Sm	5.90	5.96	3.01	0.150	1.40
Sr	271	291	243	180	103
Ta	0.497	0.478	0.296	<0.013	0.21
Tb	0.881	0.884	0.445	0.021	0.19
Th	6.43	6.37	3.37	0.158	2.88
Ti	1907	2152	1333	<106	815
U	46.9	50.2	24.1	1.03	8.94
V	227	291	114	4.65	34.2
W	1.65	1.31	0.76	<0.11	0.8
Yb	3.19	3.18	1.60	0.074	0.57
Zn	227	237	119	3.69	49
Zr	<70	<68	<0.54	<0.11	<29

Table 3. Mercury content in gypsum samples.

Sample	Mass of sample [mg]	Mass of total Hg [µg]
FF-Dry	55.7	0.58
FF-Moist	56.4	0.59
CF-Dry	56.5	0.01
CF-Moist	50.8	0.02
FF1-Dry	58.0	0.74
FF1-Moist	56.6	0.53
FF2-Dry	52.9	0.31
FF2-Moist	52.5	0.28

moist samples occur during the process of sample drying. In FF2 gypsum sample the Hg release pattern for moist and dry samples is similar (**Figure 3(d)**).

3.2.2. Gypsum Samples Spiked with Hg Compounds Mixed with CaSO$_4$·2H$_2$O

Dried fraction (FF) of gypsum was used in all subsequent experiments with spiking. The results are shown as thermograms (**Figures 4-7**) in order to facilitate and enable qualitative comparison of thermograms. In every figure four thermograms are shown where the black line represents a thermogram of the FF gypsum sample, the red one represents FF sample spiked with a particular Hg compound mixed with pure CaSO$_4$·2H$_2$O, the blue line represents a thermogram of pure Hg compound mixed with substrate CaSO$_4$·2H$_2$O, and the green represents a thermogram of pure Hg compound. Thermograms were smoothed to reduce the noise from the measuring equipment for easier comparison and clarity. The contents of total Hg in each sample are listed in **Table 4**, which also provides the information on Hg recovered in KMnO$_4$ impingers. Evidently, the recovery ranged from 70 to 100%. Losses encountered during heating may be related to evaporation loses of Hg(0), instability of some Hg compounds in air, adsorption on colder parts of the instrumentation, as well as analytical errors.

As the main intention of this work was to use thermal fractionation as a tool for identifying Hg compounds present in technical gypsum, the thermogram of the fine gypsum fraction (FF) is presented as a reference in all thermograms.

The thermograms are grouped into four subgroups including Hg halides, sulfates, oxides and HgS and HgSe for easier understanding and interpretation.

Mercury halides

Based on the presence of halogen elements (Cl, Br, F) in the WFGD system (**Table 2**) we selected Hg$_2$Cl$_2$, HgCl$_2$, HgBr$_2$ and HgF$_2$ as test compounds (**Figure 4**).

Thermograms for pure Hg chlorides and bromide are identical (**Figures 4(a)-(c)**), while that for pure HgF$_2$ differs significantly (**Figure 4(d)**), with several overlapping peaks between 200 and 370˚C and one strong peak at 440˚C [51].

The reason for similar patterns of thermograms for Hg$_2$Cl$_2$ and HgCl$_2$ lies in Hg(0) and HgCl$_2$ having the same vapor pressure [16]. At higher temperatures, Hg$_2$Cl$_2$ follows a decomposition step, described in Equation (1) where, as a result, two peaks are released (Hg(0) and HgCl$_2$) [34] [52] [53], emerging at the same temperature due to the same vapor pressure [51]. At the same temperature HgCl$_2$ compound also decomposes, following the decomposition step shown in Equation (2). Because of the similar chemical properties of Hg-Cl compounds, HgBr$_2$ decomposes at the same temperature.

$$Hg_2Cl_2 \rightarrow Hg^0 + HgCl_2 \tag{1}$$

$$HgCl_2 \rightarrow Hg^0 + Cl_2 \tag{2}$$

Owing to the HgF$_2$ high boiling and melting points and the reactivity of HF (in the presence of residual moisture) released during thermal decomposition (Equation (3)) [54], the resulting thermograms show very different patterns. The first peaks can be attributed to the decomposition of the HgF$_2$, while the second peak, at 440˚C,

corresponds to HgO decomposition as described later (**Figure 4(d)**) [51].
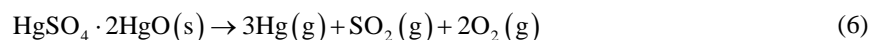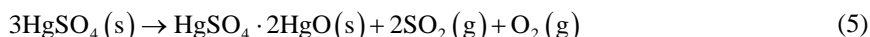
$$HgF_2 + H_2O \rightarrow HgO + 2HF \tag{3}$$

Consistent with the general observation, the thermograms of pure Hg halides and those mixed with CaSO$_4$·2H$_2$O substrate differ considerably. The released peaks of Hg from Hg$_2$Cl$_2$, HgCl$_2$ and HgBr$_2$ mixed with CaSO$_4$·2H$_2$O (**Figures 4(a)-(c)**), appearing at temperatures of around 670˚C, are difficult to explain since no theoretical background exists. We assume that this is caused by the experimental set up in which ionic Hg could have been deposited on the cooler surfaces of the inner wall of the tubing and finally released by high temperature gas flow towards the end of the temperature cycle [51]. This may be confirmed by the good mass balance observed during the experiments (**Table 4**).

The analyses of thermograms of technical gypsum (FF fraction) spiked with Hg halides show the two typical initial peaks and skewed declining trend up to 400˚C, the exception being a new clear peak at 340˚C for HgF$_2$. The relative intensities of the first two peaks in spiked and non-spiked FF gypsum are most similar for Hg$_2$Cl$_2$, and HgCl$_2$, less so for HgBr$_2$ and much less for HgF$_2$. The Hg halides can be concluded to be present in the gypsum samples with a high degree of certainty, the Hg chlorides predominating. This is in agreement with the relative concentrations of halogens in the WFGD solution [7] [34] [52] [53].

Mercury sulfates

The thermograms shown in **Figure 5** indicate some distinct differences in the decomposition patterns of Hg(I) and Hg(II) sulfates, which was not observed for Hg(I) and Hg(II) chlorides.

Pure Hg(I) sulfate (**Figure 5(a)**) shows a larger peak at 300˚C and a second at 520˚C, while Hg (II) sulfate (**Figure 5(b)**) exhibits only one major peak at 540˚C [51]. According to a report [55] this is a result of a multistep decomposition of Hg(I, II) sulfates. Decomposition of Hg$_2$SO$_4$ should follow the following decomposition steps as follows:

$$Hg_2SO_4(s) \rightarrow Hg(g) + HgSO_4(s) \tag{4}$$

$$3HgSO_4(s) \rightarrow HgSO_4 \cdot 2HgO(s) + 2SO_2(g) + O_2(g) \tag{5}$$

$$HgSO_4 \cdot 2HgO(s) \rightarrow 3Hg(g) + SO_2(g) + 2O_2(g) \tag{6}$$

The presence of pure CaSO$_4$·2H$_2$O causes a change in the appearance of the second peak for Hg(I) sulfate. A new peak appeared at 420˚C, while the second peak of pure substance Hg$_2$SO$_4$ almost disappeared. In the case of Hg(II) sulfate mixed with CaSO$_4$·2H$_2$O a new peak at around 420˚C appeared beside a strong peak with a maximum at about 560˚C. These phenomena can be explained by the change in chemistry induced by the presence of crystalline water in CaSO$_4$·2H$_2$O.

The thermograms of Hg(I) and Hg(II) sulfates mixed with technical FF gypsum differ significantly (**Figure 5(a)** and **Figure 5(b)**). In the case of Hg(I) sulfate, besides the two indicative peaks, two additional peaks ap-

Table 4. Mercury content in spiked gypsum samples.

Sample	Mass of sample [mg]	Hg-compound	Mass of Hg-spike [µg]	Mass of total Hg [µg]	Mass balance [%]
FF-Dry	50.3	Hg$_2$Cl$_2$	0.32	0.86	81.8
FF-Dry	51.3	HgCl$_2$	0.45	0.99	100
FF-Dry	88	HgBr$_2$	1.32	2.21	91.3
FF-Dry	53.0	HgF$_2$	0.77	1.39	71.9
FF-Dry	51.3	Hg$_2$SO$_4$	0.54	1.10	82.6
FF-Dry	50.6	HgSO$_4$	1.40	1.95	97.2
FF-Dry	53.6	HgO-Red	2.35	2.90	72.4
FF-Dry	50.0	HgO-Yellow	2.74	3.25	67.7
FF-Dry	50.5	HgS	3.95	4.27	93.7
FF-Dry	50.5	HgSe	2.12	2.63	93.7

peared at 260°C and 340°C but no peaks above 400°C. This observation indicates that Hg(I) sulfate is not present in the FF gypsum sample. Hg(II) sulfate, however, shows a number of non-separated peaks in the temperature range from 320 to 500°C and no peaks above 500°C. A small peak of the FF gypsum sample (black line) appears within this temperature range (with a maximum at 450°C) which indicates the possible presence of a small amount of Hg(II) sulfate in the original FF sample. This conclusion is further strengthened by the fact that only Hg(II) sulfate spiked to FF gypsum sample shows the peak within this temperature range.

Mercury oxides

Thermograms of red and yellow Hg oxides are shown in **Figure 6(a)** and **Figure 6(b)**.

Similar thermograms are observed for pure Hg oxides with maximum temperatures of 460°C and 420°C for red and yellow HgO, respectively [51]. Both HgO compounds have an orthorhombic crystalline structure but they differ in particle size [56]. Yellow HgO (**Figure 6(b)**) consists of smaller particles which may affect the decomposition temperature. A multistep decomposition of HgO is suggested [57], with the first decomposition step occurring at a temperature of 160°C - 220°C, the second at 220°C - 400°C and the third decomposition step at 400°C - 500°C. This is consistent with the results obtained in this study.

The presence of $CaSO_4 \cdot 2H_2O$ caused the release of Hg at lower temperatures, with an additional, not well separated peak at about 300°C. The effect of the matrix (substrate) on Hg release from the samples, especially from spiked gypsum samples, where Fe^{2+} and Mn^{2+} could play a role of catalysts and in the presence of Cl, could additionally enhance the reactions [7]. Thermograms of spiked FF gypsum exhibit the appearance of a maximum peak at about 350°C and 300°C for red and yellow HgO, respectively. This temperature range corresponds to the area of the not well separated skewed region of Hg release from technical FF gypsum sample. This is indicative of the presence of a small amount of HgO in FF gypsum.

Mercury sulfide and selenide

The thermograms presented in **Figure 7** show that pure compounds exhibit patterns similar to those of substrates mixed with pure compounds [51]. Major peaks for HgS (**Figure 7(a)**) appear in the range between 290 and 310°C, while for HgSe (**Figure 7(b)**) the maximum peaks appear between 250 and 290°C [51]. The decomposition temperatures for the two compounds appear in a much narrower range (within 60°C) than those for other Hg compounds, where Hg appears in much larger temperature ranges. Therefore, we can conclude that HgS and HgSe interact with the constituents of the substrate to a much lesser degree than other tested Hg compounds [51].

According to published data and without considering the fugacity effect, the decomposition temperature of HgS should be 585°C. Thus, when all factors are taken into account, a lower decomposition temperature is expected [58]. The single peak observed, is a consequence of a decomposition process of HgS consisting of only one step, which can also be termed a reactive sublimation (Equation (7)) [58].

$$HgS \rightarrow Hg + 1/2 S_2 \tag{7}$$

It has been assumed by other authors that $HgSO_3$ and HgO compounds could appear as decomposition product of HgS, which is probable when considering the gypsum produced in forced oxidation FGD. However, until now there is no evidence of such a decomposition process (Equations (8)-(10)) [32] also confirmed by our experiments.

$$HgS + 3/2 O_2 \rightarrow HgSO_3 \tag{8}$$

$$HgSO_3 \rightarrow HgO + SO_2 \tag{9}$$

$$2HgO \rightarrow 2Hg^0 + O_2 \tag{10}$$

The decomposition of pure HgSe follows just one step, according to the single released peak. It is interesting to note, that Hg and Se are among all elements far more enriched in fine fractions of the gypsum compared to lignite (**Table 2**). The enrichment factors are 110 and 88 for Se and Hg respectively. For other elements, these factors are in the range between 0.3 and 8.8. Both, Se and Hg are volatile, but highly concentrated in fine gypsum fraction, so we assumed the presence of a very stable HgSe in the gypsum. Based on the thermograms presented in **Figure 7(b)** this assumption could not be confirmed.

Both, HgS and HgSe, appear in the temperature range where the technical gypsum (FF sample, black line) shows a declining skew of Hg release with unclear peaks that cannot clearly be attributed to a specific compound tested.

More detailed analysis of all thermograms reveals that, in all cases except for HgS, those for FF gypsum spiked with different Hg compounds show two initial peaks at 170 ± 10 and $205°C \pm 5°C$. Although the oxidative environment of the WFGD system would prevent the formation of HgS in the scrubber, small amounts of H_2S present in the flue gas can produce trace amounts of highly insoluble HgS.

4. Conclusions

The results obtained in this study have confirmed previous findings that Hg is effectively retained in the WFGD system, particularly when bound to the fine fraction of the gypsum. The primary goal of this work was to identify Hg species in the gypsum using temperature fractional procedure. The methodology, however, suffers from nonspecific responses, highly dependent on the substrate in which Hg compounds are present and/or in contact with.

The thermograms of pure Hg compounds and mixtures of pure compounds with $CaSO_4 \cdot 2H_2O$ differ significantly in all cases, except for HgS and HgSe. This indicates that the release of Hg from Hg compounds during heating is importantly influenced by the presence of a substrate due to the chemical reactions occurring during heating. Furthermore, the thermograms of the fine fraction (FF) of technical gypsum spiked with the mixture of pure substance and analytical grade $CaSO_4 \cdot 2H_2O$, also differ significantly from thermograms of mixtures of pure substance and analytical grade $CaSO_4 \cdot 2H_2O$. It has to be noted, however, that the technical gypsum is a complex matrix in which Hg can be incorporated in the matrix structure in the form of different compounds and/or adsorbed on the surface of the particles. The methodology based on spiking with pure compounds applied in our work does not fully represent gypsum obtained from TPPs.

Due to the large effect of the substrate on Hg release it is decisive to use an approach based on the addition of a known Hg compound to the substrate. Detailed quantitative and qualitative analysis of Hg compounds and other constituents in gypsum is necessary for the selection of these compounds. To our knowledge the exact identification of Hg compounds in gypsum is still largely unknown. Appropriate reference materials and a reliable analytical method for speciation of Hg compounds at various concentration levels in solid samples are required.

Our results enable us to confirm that, in the gypsum obtained from a WFGD with forced oxidation, Hg halides, in particular chloride, prevail. The method used in our work cannot distinguish between Hg(I) and Hg(II) chloride. It does, however, have the potential to distinguish between Hg(I) and Hg(II) sulfates, though present at much lower levels in gypsum, of which only traces of Hg(II) sulfates were identified in the technical gypsum sample. Traces of other Hg compounds cannot fully be excluded as well.

Although, the method is not sufficiently specific for identification of the Hg species, it has proved very useful to study the temperature stability of Hg in gypsum. This stability can be altered by the addition of various substrates which may either accelerate Hg release or stabilize it. This is of importance in Hg waste characterization including of gypsum containing high Hg concentrations.

For accurate identification of Hg species, more needs to be known about the behavior of Hg compounds at higher temperatures. For accurate determination of Hg compounds present in complex matrices other, complementary, instrumental techniques could be of great help, such as for example mass spectrometry for identification of temperature decomposition fragments.

Highlights

- Hg in the coal fired TPP is effectively retained in the WFGD with forced oxidation.
- Fine gypsum fraction contains the majority of Hg and other elements.
- Identification of the Hg compounds by TF largely depends on the matrix.
- Hg in the fine gypsum fraction is mostly present as halides, primarily as chloride.

Acknowledgements

References

[1] UNEP Division of Technology, Industry and Economics, Chemicals Branch International Environment House (2013) Global Mercury Assessment 2013: Sources, Emissions, Releases and Environmental Transport. http://www.unep.org/PDF/PressReleases/GlobalMercuryAssessment2013.pdf

[2] (2013) UNEP Conference of Plenipotentiaries on the Minamata Convention on Mercury, Kumamoto, Japan, 10 and 11 October 2013. Text of the Minamata Convention on Mercury for Adoption by the Conference of Plenipotentiaries. http://www.unep.org/chemicalsandwaste/Portals/9/Mercury/Documents/dipcon/CONF_3_Minamata%20Convention%20on%20Mercury_final%2026%2008_e.pdf

[3] Galbreath, K.C. and Zygarlicke, C.J. (2000) Mercury Transformations in Coal Combustion Flue Gas. *Fuel ProcessingTechnology*, **65-66**, 289-310. http://dx.doi.org/10.1016/S0378-3820(99)00102-2

[4] Pavlish, J.H., Sondreal, E.A., Mann, M.D., Olson, E.S., Galbreath, K.C., Laudal, D.L., *et al*. (2003) Status Review of Mercury Control Options for Coal-Fired Power Plants. *Fuel Processing Technology*, **82**, 89-165. http://dx.doi.org/10.1016/S0378-3820(03)00059-6

[5] Niksa, S. and Fujiwara, N. (2005) Predicting Extents of Mercury Oxidation in Coal-Derived Flue Gases. *Journal of the Air & Waste Management Association*, **55**, 930-939. http://dx.doi.org/10.1080/10473289.2005.10464688

[6] Stergaršek, A., Horvat, M., Kotnik, J., Tratnik, J., Frkal, P., Kocman, D., *et al*. (2008) The Role of Flue Gas Desulphurisation in Mercury Speciation and Distribution in a Lignite Burning Power Plant. *Fuel*, **87**, 3504-3512. http://dx.doi.org/10.1016/j.fuel.2008.06.003

[7] Stergaršek, A., Horvat, M., Frkal, P. and Stergaršek, J. (2010) Removal of Hg-0 from Flue Gases in Wet FGD by Catalytic Oxidation with Air—An Experimental Study. *Fuel*, **89**, 3167-3177. http://dx.doi.org/10.1016/j.fuel.2010.04.006

[8] Stergaršek, A., Horvat, M., Frkal, P., Guevara, S.R. and Kocjančič, R. (2013) Removal of Hg-0 in Wet FGD by Catalytic Oxidation with Air—A Contribution to the Development of a Process Chemical Model. *Fuel*, **107**, 183-191. http://dx.doi.org/10.1016/j.fuel.2012.08.001

[9] Pudasainee, D., Kim, J.H., Yoon, Y.S. and Seo, Y.C. (2012) Oxidation, Reemission and Mass Distribution of Mercury in Bituminous Coal-Fired Power Plants with SCR, CS-ESP and Wet FGD. *Fuel*, **93**, 312-318. http://dx.doi.org/10.1016/j.fuel.2011.10.012

[10] Yan, R., Gauthier, D. and Flamant, G. (2000) Possible Interactions between As, Se, and Hg during Coal Combustion. *Combustion and Flame*, **120**, 49-60. http://dx.doi.org/10.1016/S0010-2180(99)00079-6

[11] Yudovich, Y.E. and Ketris, M.P. (2005) Mercury in Coal: A Review Part 2. Coal Use and Environmental Problems. *International Journal of Coal Geology*, **62**, 135-165. http://dx.doi.org/10.1016/j.coal.2004.11.003

[12] Ito, S., Yokoyama, T. and Asakura, K. (2006) Emissions of Mercury and Other Trace Elements from Coal-Fired Power Plants in Japan. *Science of the Total Environment*, **368**, 397-402. http://dx.doi.org/10.1016/j.scitotenv.2005.09.044

[13] Meij, R. and TeWinkel, B. (2004) The Emissions and Environmental Impact of PM10 and Trace Elements from a Modern Coal-Fired Power Plant Equipped with ESP and Wet FGD. *Fuel Processing Technology*, **85**, 641-656. http://dx.doi.org/10.1016/j.fuproc.2003.11.012

[14] Ochoa-González, R., Díaz-Somoano, M. and Martínez-Tarazona, M.R. (2013) Effect of Anion Concentrations on Hg^{2+} Reduction from Simulated Desulphurization Aqueous Solutions. *Chemical Engineering Journal*, **214**, 165-171. http://dx.doi.org/10.1016/j.cej.2012.09.037

[15] Tang, T., Xu, J., Lu, R., Wo, J. and Xu, X. (2010) Enhanced Hg^{2+} Removal and Hg^0 Re-Emission Control from Wet Fuel Gas Desulfurization Liquors with Additives. *Fuel*, **89**, 3613-3617. http://dx.doi.org/10.1016/j.fuel.2010.07.045

[16] Wu, C.L., Cao, Y., He, C.C., Dong, Z.B. and Pan, W.P. (2010) Study of Elemental Mercury Re-Emission through a Lab-Scale Simulated Scrubber. *Fuel*, **89**, 2072-2080. http://dx.doi.org/10.1016/j.fuel.2009.11.045

[17] Ochoa-González, R., Díaz-Somoano, M. and Martínez-Tarazona, M.R. (2013) Control of Hg^0 Re-Emission from Gypsum Slurries by Means of Additives in Typical Wet Scrubber Conditions. *Fuel*, **105**, 112-118. http://dx.doi.org/10.1016/j.fuel.2012.05.044

[18] Milobowski, M.G., Amrhein, G.T., Kudlac, G.A. and Yurchison, D.M. (2001) Wet FGD Enhanced Mercury Control for Coal-Fired Utility Boilers. *Proceedings of the US EPA/DOE/EPRI Combined Power Plant Air. Pollutant Control Symposium*: *The Mega Symposium*, Chicago, 20-23 August 2001.

[19] Beatty, W.L., Schroeder, K. and Beatty, C.L.K. (2012) Mineralogical Associations of Mercury in FGD Products. *Energy Fuels*, **26**, 3399-3406. http://dx.doi.org/10.1021/ef300033u

[20] Liu, X., Wang, S., Zhang, L., Wu, Y., Duan, L. and Hao, J. (2013) Speciation of Mercury in FGD Gypsum and Mercury Emission during the Wallboard Production in China. *Fuel*, **111**, 621-627. http://dx.doi.org/10.1016/j.fuel.2013.03.052

[21] Heebink, L.V. and Hassett, D.J. (2005) Mercury Release from FGD. *Fuel*, **84**, 1372-1377.

http://dx.doi.org/10.1016/j.fuel.2004.06.040

[22] Biester, H. and Scholz, C. (1996) Determination of Mercury Binding Forms in Contaminated Soils: Mercury Pyrolysis versus Sequential Extractions. *Environmental Science & Technology*, **31**, 233-239. http://dx.doi.org/10.1021/es960369h

[23] Issaro, N., Abi-Ghanem, C. and Bermond, A. (2009) Fractionation Studies of Mercury in Soils and Sediments: A Review of the Chemical Reagents Used for Mercury Extraction. *Analytica Chimica Acta*, **631**, 1-12. http://dx.doi.org/10.1016/j.aca.2008.10.020

[24] Do Valle, C.M., Santana, G.P. and Windmöller, C.C. (2006) Mercury Conversion Processes in Amazon Soils Evaluated by Thermodesorption Analysis. *Chemosphere*, **65**, 1966-1975. http://dx.doi.org/10.1016/j.chemosphere.2006.07.001

[25] Windmöller, C.C., Wilken, R.D. and Jardim, W.D. (1996) Mercury Speciation in Contaminated Soils by Thermal Release Analysis. *Water, Air, & Soil Pollution*, **89**, 399-416. http://dx.doi.org/10.1007/BF00171644

[26] Rumayor, M., Diaz-Somoano, M., Lopez-Anton, M.A. and Martinez-Tarazona, M.R. (2013) Mercury Compounds Characterization by Thermal Desorption. *Talanta*, **114**, 318-322. http://dx.doi.org/10.1016/j.talanta.2013.05.059

[27] Navarro, A., Cañadas, I., Martinez, D., Rodriguez, J. and Mendoza, J.L. (2009) Application of Solar Thermal Desorption to Remediation of Mercury-Contaminated Soils. *Solar Energy*, **89**, 1405-1414. http://dx.doi.org/10.1016/j.solener.2009.03.013

[28] Coufalík, P., Zvěřina, O. and Komárek, J. (2014) Determination of Mercury Species Using Thermal Desorption Analysis in AAS. *Chemical Papers*, **68**, 427-434. http://dx.doi.org/10.2478/s11696-013-0471-0

[29] Coufalík, P., Krásenský, P., Dosbaba, M. and Komárek, J. (2012) Sequential Extraction and Thermal Desorption of Mercury from Contaminated Soil and Tailings from Mongolia. *Central European Journal of Chemistry*, **10**, 1565-1573. http://dx.doi.org/10.2478/s11532-012-0074-6

[30] Rallo, M., Lopez-Anton, M.A., Perry, R. and Maroto-Valer, M.M. (2010) Mercury Speciation in Gypsums Produced from Flue Gas Desulfurization by Temperature Programmed Decomposition. *Fuel*, **89**, 2157-2159. http://dx.doi.org/10.1016/j.fuel.2010.03.037

[31] Murakami, A., Uddin, M.A., Ochiai, R., Sasaoka, E. and Wu, S. (2010) Study of the Mercury Sorption Mechanism on Activated Carbon in Coal Combustion Flue Gas by the Temperature-Programmed Decomposition Desorption Technique. *Energy & Fuels*, **24**, 4241-4249. http://dx.doi.org/10.1021/ef100288f

[32] Wu, S., Uddin, M.A., Nagano, S., Ozaki, M. and Sasaoka, E. (2011) Fundamental Study on Decomposition Characteristics of Mercury Compounds over Solid Powder by Temperature-Programmed Decomposition Desorption Mass Spectrometry. *Energy & Fuels*, **25**, 144-153. http://dx.doi.org/10.1021/ef1009499

[33] Raposo, C., Windmöller, C.C. and Durao Jr., W.A. (2003) Mercury Speciation in Fluorescent Lamps by Thermal Release Analysis. *Waste Management*, **23**, 879-886. http://dx.doi.org/10.1016/S0956-053X(03)00089-8

[34] Lopez-Anton, M.A., Yuan, Y., Perry, R. and Maroto-Valer, M.M. (2010) Analysis of Mercury Species Present during Coal Combustion by Thermal Desorption. *Fuel*, **89**, 629-634. http://dx.doi.org/10.1016/j.fuel.2009.08.034

[35] Luo, G., Yao, H., Xu, M., Gupta, R. and Xu, Z. (2011) Identifying Modes of Occurrence of Mercury in Coal by Temperature Programmed Pyrolysis. *Proceedings of the Combustion Institute*, **33**, 2763-2769. http://dx.doi.org/10.1016/j.proci.2010.06.108

[36] Shuvaeva, O.V., Gustaytis, M.A. and Anoshin, G.N. (2008) Mercury Speciation in Environmental Solid Samples Using Thermal Release Technique with Atomic Absorption Detection. *Analytica Chimica Acta*, **621**, 148-154. http://dx.doi.org/10.1016/j.aca.2008.05.034

[37] Biester, H., Müller, G. and Schöler, H.F. (2002) Binding and Mobility of Mercury in Soils Contaminated by Emissions from Chlor-Alkali Plants. *Science of the Total Environment*, **284**, 191-203. http://dx.doi.org/10.1016/S0048-9697(01)00885-3

[38] Bollen, A., Wenke, A. and Biester, H. (2008) Mercury Speciation Analyses in HgCl$_2$-Contaminated Soils and Groundwater—Implications for Risk Assessment and Remediation Strategies. *Water Research*, **42**, 91-100. http://dx.doi.org/10.1016/j.watres.2007.07.011

[39] Biester, H., Gosar, M. and Müller, G. (1999) Mercury Speciation in Tailings of the Idrija Mercury Mine. *Journal of Geochemical Exploration*, **65**, 195-204. http://dx.doi.org/10.1016/S0375-6742(99)00027-8

[40] Ochoa-Gonzalez, R., Diaz-Somoano, M. and Martinez-Tarazona, M.R. (2013) Influence of Limestone Characteristics on Mercury Re-Emission in WFGD Systems. *Environmental Science & Technology*, **47**, 2974-2981. http://dx.doi.org/10.1021/es304090e

[41] Kairies, C., Schroeder, K. and Cardone, C. (2006) Mercury in Gypsum Produced from Flue Gas Desulfurization. *Fuel*, **85**, 2530-2536. http://dx.doi.org/10.1016/j.fuel.2006.04.027

[42] Cornell, R.M. and Schwertmann, U. (2003) The Iron Oxides: Structure, Properties, Reactions, Occurrences and Uses. 2nd Edition, Wiley-VCH, Weinheim. http://dx.doi.org/10.1002/3527602097

[43] Kim, C.S., Rytuba, J.J. and Brown, G.E. (2004) EXAFS Study of Mercury(II) Sorption to Fe- and Al-(Hydr)oxides. *Journal of Colloid and Interface Science*, **270**, 9-20. http://dx.doi.org/10.1016/j.jcis.2003.07.029

[44] Evans, M.A. and Elmore, R.D. (2006) Fluid Control of Localized Mineral Domains in Limestone Pressure Solution Structures. *Journal of Structural Geology*, **28**, 284-301. http://dx.doi.org/10.1016/j.jsg.2005.10.004

[45] Kotnik, J., Horvat, M., Mandić, V. and Logar, M. (2000) Influence of the Šoštanj Coal-Fired Thermal Power Plant on Mercury and Methyl Mercury Concentrations in Lake Velenje, Slovenia. *Science of the Total Environment*, **259**, 85-95. http://dx.doi.org/10.1016/S0048-9697(00)00576-3

[46] Akagi, H. and Nishimura, H. (1991) Speciation of Mercury in the Environment. In: Suzuki, T., Imura, N. and Clarkson, T.W., Eds., *Advances in Mercury Toxicology*, Plenum Press, New York, 53-76. http://dx.doi.org/10.1007/978-1-4757-9071-9_3

[47] Jaćimović, R., Smodiš, B., Bučar, T. and Stegnar, P. (2003) K_0-NAA Quality Assessment by Analysis of Different Certified Reference Materials Using the KAYZERO/SOLCOI Software. *Journal of Radioanalytical and Nuclear Chemistry*, **257**, 659-663. http://dx.doi.org/10.1023/A:1026116916580

[48] Smodiš, B., Jaćimović, R., Medin, G. and Jovanović, S. (1993) Instrumental Neutron Activation Analysis of Sediment Reference Materials Using the K_0-Standardisation Method. *Journal of Radioanalytical and Nuclear Chemistry*, **169**, 177-185. http://dx.doi.org/10.1007/BF02046792

[49] Kayzero for Windows (KayWin®), User's Manual for Reactor Neutron Activation Analysis (NAA) Using the K_0 Standardization Method, Version 2, November 2005.

[50] Sholupov, S., Pogarev, S., Ryzhov, V., Mashyanov, N. and Stroganov, A. (2004) Zeeman Atomic Absorption Spectrometer RA-915+ for Direct Determination of Mercury in Air and Complex Matrix Samples. *Fuel Processing Technology*, **85**, 473-485. http://dx.doi.org/10.1016/j.fuproc.2003.11.003

[51] Sedlar, M., Pavlin, M., Popovič, A. and Horvat, M. (2015) Temperature Stability of Mercury Compounds in Solid Substrates. *Open Chemistry*, **13**, 404-419.

[52] Acuña-Caro, C., Brechtel, K., Scheffknecht, G. and Braß, M. (2009) The Effect of Chlorine and Oxygen Concentrations on the Removal of Mercury at an FGD-Batch Reactor. *Fuel*, **88**, 2489-2494. http://dx.doi.org/10.1016/j.fuel.2008.11.028

[53] Blythe, G., DeBerry, D., Marsh, B., Paradis, J., Range, J. and Rhudy, R. (2004) Bench-Scale Evaluation of the Fate of Mercury in Wet FGD Systems. *Proceedings of the Air and Waste Management Association's Combined Power Plant Air Pollution Control Mega Symposium*, Washington DC, 30 August-2 September 2004, Paper No. 59.

[54] Guminski, C. (2001) The F-Hg System (Fluorine-Mercury). *Journal of Phase Equilibria*, **22**, 578-581. http://dx.doi.org/10.1007/s11669-001-0084-0

[55] Tariq, S.A. and Hill, J.O. (1981) Thermal Analysis of Mercury(I) Sulfate and Mercury(II) Sulphate. *Journal of Thermal Analysis*, **21**, 277-281. http://dx.doi.org/10.1007/BF01914211

[56] Wendlandt, W.W. (1974) Thermal Properties of Inorganic Compounds. Hg(I) Hg(II) Compounds. *Thermochimica Acta*, **10**, 101-107. http://dx.doi.org/10.1016/0040-6031(74)85028-8

[57] L'vov, B.V. (1999) Kinetics and Mechanisms of Thermal Decomposition of Mercuric Oxide. *Thermochimica Acta*, **333**, 21-26. http://dx.doi.org/10.1016/S0040-6031(99)00086-6

[58] Leckey, J.H. and Nulf, L.E. (1994) Thermal Decomposition of Mercuric Sulfide. Chemistry and Chemical Engineering Department—Development Organization. Oak Ridge Y-12 Plant. Martin Marietta Energy Systems, Inc., US Department of Energy, Tennessee. http://dx.doi.org/10.2172/41313